Available online at www.sciencedirect.com
ScienceDirect
C. R. Chimie 12 (2009) 772–778
COMPTES RENDUS CHIMIE

Full paper / Mémoire

Investigation of the effect of support thermal treatment on gold-based catalysts' activity towards propene total oxidation

Mohamed Lamallem, Renaud Cousin*, Rudy Thomas, Stéphane Siffert, Faustin Aïssi, Antoine Aboukaïs

Laboratoire de catalyse et environnement, EA 2598, Université du Littoral Côte d'Opale, 145, avenue Maurice-Schumann, 59140 Dunkerque, France

Received 3 June 2008; accepted after revision 20 October 2008
Available online 3 March 2009

Abstract

This paper reports a study on the effect of support thermal treatment on the activity of gold-based catalysts for the total oxidation of propene. $Ce_{0.3}Ti_{0.7}O_2$ supports were prepared using sol–gel method. These compounds are calcined at 400, 500 and 600 °C. Physico-chemical properties of synthesized materials were characterized by means of XRD, DR/UV–vis and H_2-TPR. Then gold was deposited on these supports by the deposition precipitation method. Thus the catalytic activity of these solids in the propene oxidation was evaluated. On the basis of the catalytic results, a better activity is obtained when gold is deposited on $Ce_{0.3}Ti_{0.7}O_2$ support previously calcined at 400 °C under air. ***To cite this article: M. Lamallem et al., C. R. Chimie 12 (2009).***

Résumé

Ce manuscrit décrit une étude concernant l'influence du traitement thermique du support sur l'activité de catalyseurs à base d'or pour l'oxydation totale du propène. Des supports oxydes ($Ce_{0.3}Ti_{0.7}O_2$) ont été synthétisés par la méthode sol–gel puis calcinés à 400, 500 et 600 °C. Les propriétés physico-chimiques de ces matériaux ont été étudiées par DRX, UV–vis en réflexion diffuse et par H_2-RTP. Ensuite, l'or a été déposé sur ces supports par la méthode « dépôt-précipitation ». L'activité catalytique de ces solides a pu être évaluée dans l'oxydation totale du propène. Ainsi, lorsque l'or a été déposé sur un support $Ce_{0.3}Ti_{0.7}O_2$ calciné à 400 °C, une meilleure activité a été observée. ***Pour citer cet article : M. Lamallem et al., C. R. Chimie 12 (2009).***

Keywords: Cerium; Titanium; Gold; Catalyst; Propene oxidation

Mots-clés : Cérium ; Titane ; Or ; Catalyseur ; Oxydation du propène

1. Introduction

The decrease of the air quality in the last two decades has prompted the emergence of stricter regulations covering automotive and industrial activities.

* Corresponding author.
E-mail address: Renaud.Cousin@univ-littoral.fr (R. Cousin).

1631-0748/$ - see front matter © 2009 Académie des sciences. Published by Elsevier Masson SAS. All rights reserved.
doi:10.1016/j.crci.2008.10.022

Among these, the reduction of volatile organic compounds (VOCs) is particularly important because VOCs represent a serious environmental problem. The deep catalytic oxidation of these pollutants to carbon dioxide and water has been identified as one of the most efficient ways to destroy VOCs at low concentrations.

Catalytic systems containing highly dispersed gold particles have received a great interest, due to their high catalytic activity, particularly in CO oxidation even at room temperature [1–4]. Recently, it was shown that gold catalysts are efficient in the total oxidation of VOCs [5–7]. Moreover, we have shown in previous works [8,9], that it seems to be interesting to combine the physico-chemical properties of gold, cerium and titanium in order to obtain a suitable catalytic material for the total oxidation of VOCs. The catalytic activity and stability of gold-based compounds depend on the nature of the support, the size and distribution of gold particles and the properties of the gold support contact surface. The surface properties of the supports affect the final dispersion of gold nanoparticles and therefore their catalytic performance. Moreau and Bond [10] have prepared gold catalysts using anatase TiO_2 support with specific surface area between 10 and 350 $m^2\,g^{-1}$. They reported the influence of the surface area of the support on the activity of gold catalysts for CO oxidation. However, little information is known about the effect of the support thermal treatment on the reactivity towards the total VOC oxidation.

Thus, the aim of this work is to study the effect of support thermal treatment on the activity of gold catalysts for the total oxidation of propene. Propene was chosen as probe molecule for the catalytic oxidation, because it is often found in industrial exhausts and presents high photochemical ozone creation potentials (POCP) [11]. The oxide support and the gold catalysts have been characterized by various techniques, such as BET, XRD, DR/UV–vis and H_2-TPR, and attempts have been made to correlate the catalytic activity with the physico-chemical properties of the solids.

2. Experimental

2.1. Catalyst preparation

Ce–Ti oxide ($Ce_{0.3}Ti_{0.7}O_2$) was synthesized using the sol–gel method [12,13]. Desired amount of an aqueous solution of cerium nitrate $Ce(NO_3)_3\cdot 6H_2O$ [Rectapur, 99.5%] and ethanol CH_3CH_2OH were added under stirring to another solution of ethanol CH_3CH_2OH and titanium(IV) isopropoxide $Ti(OC_3H_7)_4$ [Across Organics; 98%] with molar ratio $Ti(OC_3H_7)_4/CH_3CH_2OH = 1/2$. The molar ratio between H_2O and titanium(IV) precursor is $H_2O/Ti(OC_3H_7)_4 = 5$. The solution was gelled after finishing the reaction between titanium(IV) isopropoxide $Ti(OC_3H_7)_4$ and water. The gel was dried at 80 °C during 24 h.

To investigate the effect of the calcination temperatures on the properties of $Ce_{0.3}Ti_{0.7}O_2$ oxide, the dried solid was calcined under air for 4 h at different temperatures: 400, 500 and 600 °C. These samples are denoted as $Ce_{0.3}Ti_{0.7}O_2$ (calc. *T*), where *T* indicates the calcination temperature.

The gold-based catalysts were prepared by the deposition precipitation (DP) method [14]. Aqueous solution of tetrachloroauric acid (10^{-3} mol L^{-1}) [Stremchemicals; 99.9%] was added under stirring to an aqueous suspension of oxide support $Ce_{0.3}Ti_{0.7}O_2$ and aqueous solution of urea in excess. The solution was heated at 80 °C to decompose urea and obtain pH equal to 6.7. The pH of solution was maintained at the value of 6.7 during 4 h to obtain high dispersion of fine gold particles on the oxide supports. The mixture was filtered and washed with deionised water at 60 °C several times in order to eliminate the chloride ions, dried during 24 h at 80 °C and finally calcined under air for 4 h at 400 °C. The catalyst thus obtained are denoted as $Au/Ce_{0.3}Ti_{0.7}O_2$ (calc. *T*), where *T* is the calcination temperature of the support.

2.2. Catalyst characterization

Elemental analyses were performed by inductively coupled plasma atomic emission spectroscopy at the CNRS Centre of Chemical Analysis (Vernaison, France).

BET surface area was measured by nitrogen adsorption at −196 °C in a Thermo-Electron QSurf M1 apparatus. Before analysis, the samples were treated for 30 min at 120 °C under a 30% N_2/He flow.

XRD analysis was performed on a BRUKER Advance D8 powder X-ray diffractometer using Cu Kα radiation. Diffraction patterns were recorded over a 2θ range of 15–80° and using a step size of 0.02° and a step time of 4 s. The mean crystallite sizes were estimated using the Scherrer equation.

Diffuse Reflectance UV–vis spectroscopy (DR/UV–vis) experiments were carried out on a VARIAN CARY 5000. The measurements were performed on air exposed samples at ambient temperature between 200 and 800 nm.

The temperature programmed reduction experiments were carried out in an Altamira AMI-200 apparatus. The TPR profiles were obtained by passing a 5% H_2/Ar flow (30 mL min^{-1}) through 50 mg of samples heated at 5 °C min^{-1} from ambient temperature to 900 °C. The hydrogen concentration in the effluent was continuously monitored by a thermo-conductivity detector (TCD).

2.3. Catalytic activity measurements

Catalytic tests were carried out at atmospheric pressure in a conventional fixed bed microreactor using 100 mg of fine catalyst powder. The reactive flow (100 mL min^{-1}) is composed of air and 6000 ppm of propene. The reactants and the reaction products were analysed by a VARIAN chromatograph equipped with FID and TCD detectors. The catalysts were first activated at 400 °C for 4 h under air (2 L h^{-1}) and the conversion measurement was studied on a slow heating ramp between 20 and 400 °C at 1 °C min^{-1}. The temperature ramp of 1 °C min^{-1} was considered to be slow enough to reach a pseudo-steady state at every point.

3. Results and discussion

3.1. $Ce_{0.3}Ti_{0.7}O_2$ oxide study

Fig. 1 presents the conversion of propene as a function of temperature in the presence of the catalytic support $Ce_{0.3}Ti_{0.7}O_2$ calcined at different temperatures. It can be observed that the catalytic activity of mixed oxides is quite similar whatever the calcination temperature of supports. Over none of these oxides 100% conversion was reached. However, regarding the conversion rate of propene at 400 °C in Table 1, a slightly better activity of the $Ce_{0.3}Ti_{0.7}O_2$ support calcined under air at 400 °C can be noticed. In order to identify the physico-chemical properties of these samples, these materials were characterized by several techniques.

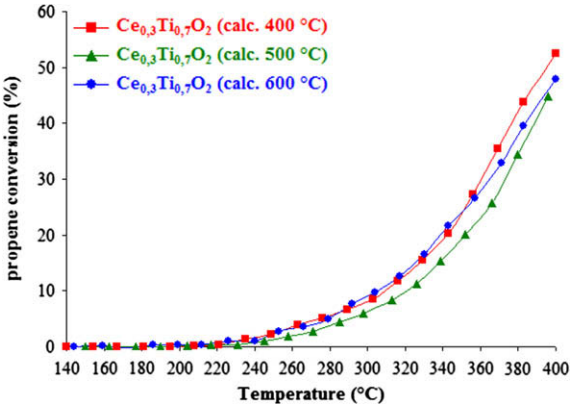

Fig. 1. Propene conversion versus temperature over $Ce_{0.3}Ti_{0.7}O_2$ supports calcined at 400, 500 and 600 °C.

BET specific surface area of the samples calcined at 400, 500 and 600 °C are mentioned in Table 1. The surface area decreases with increasing calcination temperature. Regarding the activity measurement, it can be observed that the solid $Ce_{0.3}Ti_{0.7}O_2$ (calc. 400 °C) which present the best activity, possess the highest specific area (230 m^2 g^{-1}).

XRD patterns of the $Ce_{0.3}Ti_{0.7}O_2$ support at different calcination temperatures are reported in Fig. 2. This figure shows that all the samples are characterized by the absence of well resolved diffraction peaks of TiO_2 or CeO_2. This indicates that the solids are in a relatively amorphous state. The highly amorphous character of the samples can be deduced from the high level of noise detected in the patterns. Thus, for the sample $Ce_{0.3}Ti_{0.7}O_2$ calcined at 400 and 500 °C a broad peak at around $2\theta = 28.5°$ is observed on their XRD profiles. However, when the solid was calcined at 600 °C, some patterns with bad resolution corresponding to anatase and cerianite phases are revealed. This result indicates that some CeO_2 and TiO_2 crystallites are present in the $Ce_{0.3}Ti_{0.7}O_2$ (calc. 600 °C) sample. This is in accordance with the BET measurement; which reveals the lowest value (86 m^2 g^{-1}) for this solid, due to its higher degree of crystallinity than the other samples. The same behavior has been observed by Rynkowski et al. [12] in the case of ceria–titania mixed oxides with atomic ratios Ti/Ce = 8/2. Lopez et al. [15] have evidenced the appearance of well resolved diffraction lines of cerianite phase in the mixed oxide TiO_2–CeO_2 (90 wt% of TiO_2) after calcination at 800 °C. Those authors have shown that the ceria is formed at low temperature

Table 1
Calcination temperature, BET specific area and propene conversion, over $Ce_{0.3}Ti_{0.7}O_2$ supports calcined at 400, 500 and 600 °C.

Support	Calcination temperature (°C)	S_{BET} (m^2/g)	Conversion rate at 400 °C
$Ce_{0.3}Ti_{0.7}O_2$ (calc. 400 °C)	400	230	55
$Ce_{0.3}Ti_{0.7}O_2$ (calc. 500 °C)	500	190	49
$Ce_{0.3}Ti_{0.7}O_2$ (calc. 600 °C)	600	86	48

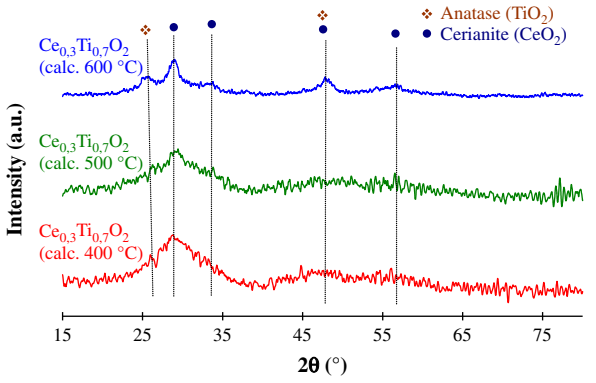

Fig. 2. XRD patterns of $Ce_{0.3}Ti_{0.7}O_2$ supports calcined at 400, 500 and 600 °C.

in the form of small dispersed crystallites in the structure of amorphous TiO_2 and which are not detected by the XRD. When increasing the calcination temperature, these crystallites start growing and sintering to constitute larger ones, which allow their detection. Indeed the better crystallization state is in accordance with the decrease of the specific areas of the $Ce_{0.3}Ti_{0.7}O_2$ samples when increasing the calcination temperature to 600 °C.

DR/UV–vis optical spectra of $Ce_{0.3}Ti_{0.7}O_2$ samples are reported in Fig. 3. Several absorption bands characteristic of titanium are observed in the range 200–400 nm. According to the literature [16–18], the band at 215 nm should be due to isolated Ti(IV) in a tetra-coordinated environment, the band at 220 nm is attributed to isolated Ti atoms in octahedral coordination, the band at 260 nm is attributed to Ti^{4+} ions in octahedral coordination. The peak at 330 nm is ascribed to the $O^{2-} \rightarrow Ti^{4+}$ charge transfer transition, indicating the anatase TiO_2 species. The band observed at 300 nm is attributed to $O^{2-} \rightarrow Ce^{4+}$ charge transfer transition [19]. When increasing the calcination temperature, the adsorption edge at 380 nm assigned to the inter-band transitions which take place in CeO_2 shifts to the visible range. Several studies [20,21] have shown that increasing the size of semi-conducting micro-crystallites entails a shift of the absorbance edge of the inter-band transition. This result is in accordance with XRD analysis which presents the formation of crystallites of ceria with the increase of the calcination temperature of the solids.

Fig. 4 shows the profiles obtained after H_2-TPR measurements of $Ce_{0.3}Ti_{0.7}O_2$ calcined at various temperatures. For all oxides, a first broad peak starting at about 280 °C is detected. This reduction peak maximum shifts from 466 to 545 °C with increasing calcination temperature from 400 to 600 °C. In accordance with literature data [13,22], this reduction peak is generally attributed to reduction of oxygen species in the surface region of ceria whereas the very small peak observed at about 790 °C corresponds to the reduction of the oxygen species in the bulk of the ceria. The shift of the low temperature reduction peak to a higher temperature could be induced by the formation and agglomeration of nanoparticles of Ceria and Titania. Indeed, Mengfei et al. [13] have shown that with the increasing of the temperature, the H_2-TPR peak shifts to higher temperatures, probably, because of the sintering of the samples. The hydrogen consumption is also presented in Table 2. It could be observed that the H_2 consumption is relatively constant, whatever is the calcination temperature of the Ce–Ti oxides.

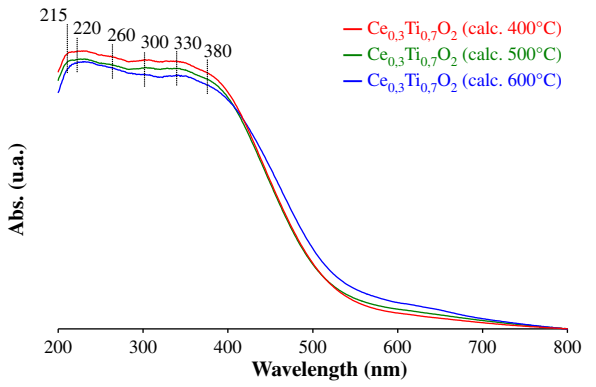

Fig. 3. DR/UV–vis spectra of $Ce_{0.3}Ti_{0.7}O_2$ supports calcined at 400, 500 and 600 °C.

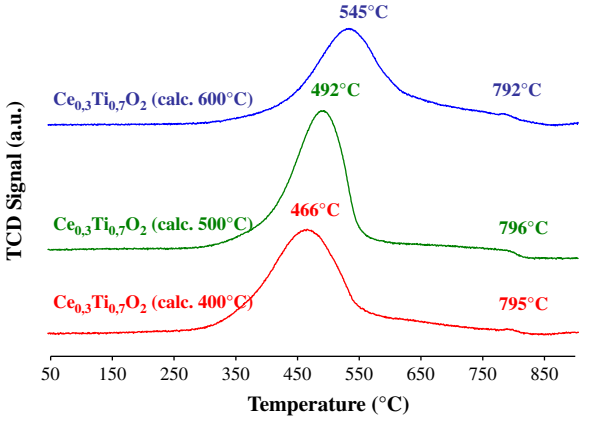

Fig. 4. H_2-TPR profiles of $Ce_{0.3}Ti_{0.7}O_2$ supports calcined at 400, 500 and 600 °C.

Table 2
Reduction peak position and H_2 consumption over $Ce_{0.3}Ti_{0.7}O_2$ supports calcined at 400, 500 and 600 °C.

Support	Temperature of 1st reduction peak (°C)	Hydrogen consumption (μmol g^{-1})
$Ce_{0.3}Ti_{0.7}O_2$ (calc. 400 °C)	466	1129
$Ce_{0.3}Ti_{0.7}O_2$ (calc. 500 °C)	492	1124
$Ce_{0.3}Ti_{0.7}O_2$ (calc. 600 °C)	545	1171

3.2. *Au/$Ce_{0.3}Ti_{0.7}O_2$ catalysts' study*

Gold is deposited on calcined oxides as described in Experimental section. The gold content (% wt) determined by elemental analysis is mentioned in Table 3.

Fig. 5 represents the conversion of propene as a function of temperature in the presence of different gold-based catalysts. Thus, adding gold on the oxide support improves the catalytic activity for the propene oxidation. The propene conversion is performed at lower temperature and presents 100% of selectivity towards formation of CO_2. It can be observed that the catalytic activity changes slightly according to the temperature of support calcination. It seems that the gold deposited on support calcined at 400 °C presents the best catalytic activity. Thus, the calcination temperature of the support seems to have an effect in the activity for gold-catalyzed propene oxidation.

Concerning the BET measurement (Table 3), a slight decrease in surface area was observed when gold is deposited on the support. Moreover, it can be noticed that the catalyst with the support calcined at 400 °C exhibits the highest surface area and the best catalytic activity towards propene oxidation.

The XRD patterns for the gold-based catalysts are given in Fig. 6. No change concerning the structure of the $Ce_{0.3}Ti_{0.7}O_2$ support due to the gold deposition has been evidenced. However, a small diffraction peak at $2\theta = 38.3°$ appears for all samples. This peak corresponds to nanoparticles of metallic gold. The size of the gold particles, deduced from the broadening of this

Table 3
Gold content and BET specific area of $Au/Ce_{0.3}Ti_{0.7}O_2$ catalysts.

Catalyst	Gold content (% wt)	S_{BET} (m^2/g)
$Au/Ce_{0.3}Ti_{0.7}O_2$ (calc. 400 °C)	3.07	215
$Au/Ce_{0.3}Ti_{0.7}O_2$ (calc. 500 °C)	2.97	171
$Au/Ce_{0.3}Ti_{0.7}O_2$ (calc. 600 °C)	3.30	86

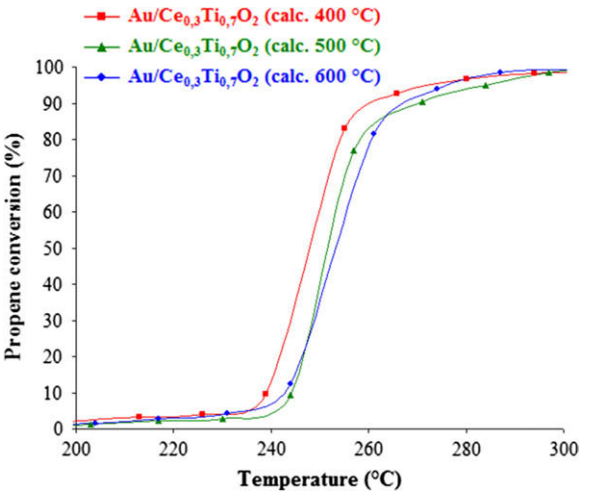

Fig. 5. Propene conversion versus temperature over $Au/Ce_{0.3}Ti_{0.7}O_2$ catalysts.

reflexion peak is evaluated. Their values are 9, 12, and 7 nm for catalysts with the support calcined at 400, 500 and 600 °C, respectively.

In order to identify the nature of the active gold particles, the catalysts were analysed by DR/UV–vis spectrophotometry. The obtained spectra are represented in Fig. 7. Besides, the support contribution, the UV–vis spectra of the gold-based catalyst show a new band at around 560 nm. The observation of this absorption peak is corresponding to metallic gold nanoparticules. This phenomenon has also been revealed in previous work [9]. This band is characteristic of surface plasmon resonance of metallic gold particles which arises from the collective oscillations of the free conduction band electrons that are induced by the incident electromagnetic radiation. Such resonances are observed when the wavelength of the

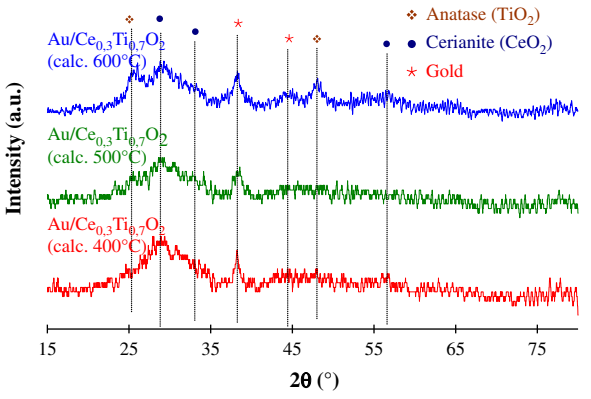

Fig. 6. XRD patterns of $Au/Ce_{0.3}Ti_{0.7}O_2$ catalysts.

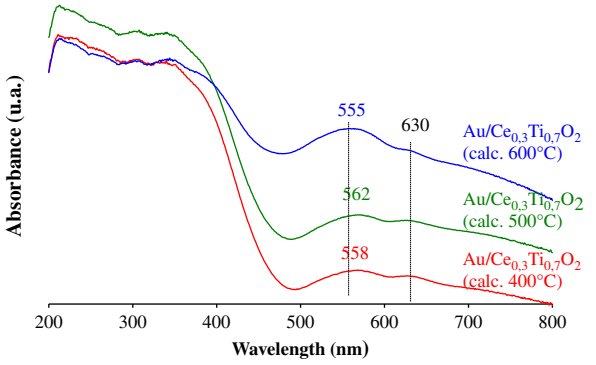

Fig. 7. DR/UV–vis spectra of $Au/Ce_{0.3}Ti_{0.7}O_2$ catalysts.

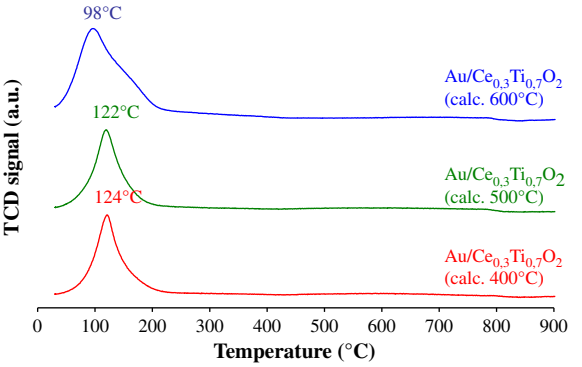

Fig. 8. H_2-TPR profiles of $Au/Ce_{0.3}Ti_{0.7}O_2$ catalysts.

incident light far exceeds the particle diameter. The small variations of wavelength of this type of bands are dependent on particle size, shape, and surrounding environment [14,23–25]. Moreover, it is interesting to note that another absorption band at around 630 nm appeared which belongs to the longitudinal plasmon resonance band of aggregates or deviation from spherical geometry [26–28] of gold nanoparticles.

The H_2-TPR profiles of the gold deposited $Ce_{0.3}Ti_{0.7}O_2$ supports represented in Fig. 8 show a reduction peak at low temperature. The TPR profile of the $Ce_{0.3}Ti_{0.7}O_2$ represented in Fig. 4 shows a massif peak of reduction in the range of 466–545 °C, this one is attributed to the reduction of surface oxygen species from ceria. When gold is added to the support, modification in the TPR profiles was observed. Indeed a reduction peak appears at lower temperature. This peak corresponds to the reduction of the oxygen species on the gold particles and on ceria. Andreeva et al. [29,30] have shown that adding noble metals (like gold) on CeO_2 permits to lower the reduction temperature of oxygen species on ceria surface. Table 4 resumes the H_2-TPR experimental and calculated consumption of catalyst samples for peaks at low temperature (<400 °C). For the H_2 calculated consumption, we consider that gold species are in the ionic state Au^{3+}. Thus, knowing the gold content in solids and following the reduction reaction of Au^{3+} into Au^0, the amount of H_2 over consumption by the catalysts could be estimated. The H_2 over consumption exists for all gold catalysts. This result shows the influence of gold to facilitate the reduction of oxygen species from $Ce_{0.3}Ti_{0.7}O_2$ support surface on the border with gold. These results could be correlated to the results of the catalytic tests. Indeed, it can be noticed that the solid named $Au/Ce_{0.3}Ti_{0.7}O_2$ (Calc. 400 °C) shows the best activity towards the total oxidation of propene, showing also higher hydrogen over consumption. This observation could be explained by the interaction between gold nanoparticles and cerium oxide. Ceria is very well known for its oxygen storage capacity (OSC), defined as the capacity to release and accept oxygen. Centeno et al. [6] have studied the catalytic combustion of VOCs on $Au/CeO_x/Al_2O_3$, and they concluded that the presence of cerium ions has a positive influence on the fixation and the final dispersion of gold on alumina support. Moreover, ceria stabilizes the gold particles with low crystallite size. In addition to these beneficial features, ceria, because of its redox properties, may improve the catalytic behavior of the catalyst by increasing the supply of active oxygen. Similar conclusions were proposed by Sciré et al. [22] in their study of VOC oxidation over Au/CeO_2. The mechanism of hydrocarbon oxidation over ceria and other reducible metal oxides is usually considered to be of the redox or Mars

Table 4
Gold reduction peak position and H_2 consumption as a function of $Au/Ce_{0.3}Ti_{0.7}O_2$ catalysts.

Catalyst	Temperature programmed reduction			
	Peak position (°C)	Calculated H_2 consumption $Au^{3+} \rightarrow Au^0$ (μmol g^{-1})	Experimental H_2 consumption (μmol g^{-1})	H_2 over consumption (μmol g^{-1})
$Au/Ce_{0.3}Ti_{0.7}O_2$ (calc. 400 °C)	124	233.8	1190	956.2
$Au/Ce_{0.3}Ti_{0.7}O_2$ (calc. 500 °C)	122	226.2	1169	942.8
$Au/Ce_{0.3}Ti_{0.7}O_2$ (calc. 600 °C)	98	251.3	1182	930.8

and van Krevelen type [6,22]. The key steps of this mechanism are believed to be the supply of active oxygen by the readily reducible oxide and its reoxidation by oxygen. Gluhoi et al. [7] have shown that gold-based catalysts that contain a transition metal oxide or ceria are highly active in propene oxidation. The role of the oxide is twofold: it stabilizes the gold particles against sintering (ceria) and provides active oxygen for the reaction.

4. Conclusion

$Ce_{0.3}Ti_{0.7}O_2$ solids were prepared using the sol–gel method. These compounds are calcined at 400, 500 and 600 °C. Gold was deposited on this support by the deposition precipitation method. Then the catalytic activity of these solids in the propene oxidation was evaluated. On the basis of the catalytic results, a better activity is obtained for gold-based catalyst when $Ce_{0.3}Ti_{0.7}O_2$ support was previously calcined at 400 °C under air.

The XRD study allowed us to identify various crystalline phases present in the solids. It also revealed the presence of fine metallic gold particles whose size has been estimated in the range of 7–12 nm. In addition, the DR/UV–vis study revealed the presence of a band at around 560 nm. This band is characteristic of the surface plasmon resonance of monodispersed metallic gold nanoparticles, which is consistent with the XRD study.

The physico-chemical study of the solids reveals that the deposition of fine metallic gold nanoparticles on the $Ce_{0.3}Ti_{0.7}O_2$ support previously calcined at 400 °C seems to play an important role for the reactivity towards the propene total oxidation.

Acknowledgements

The authors would like to thank the Urban Community of Dunkerque for the financial assistance allocated for the purchases of the UV–vis spectrophotometer and the specific area measurement apparatus. The ‘‘Conseil General du Nord’’, the ‘‘Region Nord-Pas de Calais’’ and the European Community (European Regional Development Fund) are gratefully acknowledged for financial support.

References

[1] M. Haruta, S. Tsubota, T. Kobayashi, H. Kageyama, M.J. Genet, B. Delmon, J. Catal. 144 (1993) 175.
[2] G.C. Bond, Catal. Today 72 (2002) 5.
[3] I. Dobrosz, K. Jiratova, V. Pitchon, J.M. Rynkowski, J. Mol. Catal. A 234 (2005) 187.
[4] M. Daté, M. Haruta, J. Catal. 201 (2001) 221.
[5] R.J.H. Grisel, B.E. Nieuwenhuys, Catal. Today 64 (2001) 69.
[6] M.A. Centeno, M. Paulis, M. Montes, J.A. Odriozola, Appl. Catal. A 234 (2002) 65.
[7] A.C. Gluhoi, N. Bogdanchikova, B.E. Nieuwenhuys, J. Catal. 232 (2005) 96.
[8] C. Gennequin, M. Lamallem, R. Cousin, S. Siffert, F. Aïssi, A. Aboukaïs, Catal. Today 122 (2007) 301.
[9] M. Lamallem, H. El Ayadi, C. Gennequin, R. Cousin, S. Siffert, F. Aïssi, A. Aboukaïs, Catal. Today 137 (2008) 367.
[10] F. Moreau, G.C. Bond, Catal. Today 122 (2007) 215.
[11] R.G. Derwent, M.E. Jenkin, S.M. Saunders, M.J. Pilling, Atmos. Environ. 32 (1998) 2429.
[12] J. Rynkowski, J. Farbotko, R. Touroude, L. Hilaire, Appl. Catal. A 203 (2000) 335.
[13] L. Mengfei, C. Jun, C. Linshen, L. Jiqing, F. Zhaochi, L. Can, Chem. Mater. 13 (2001) 197.
[14] R. Zanella, S. Giorgio, C. Shin, C.R. Henry, C. Louis, J. Catal. 222 (2004) 357.
[15] T. Lopez, F. Rojas, R.A. Katez, F. Galindo, A. Balankin, A. Buljan, J. Solid State Chem. 177 (2004) 1873.
[16] T. Blasco, A. Corma, M.T. Nauvarro, J.P. Pariente, J. Catal. 156 (1995) 65.
[17] B.S. Uphade, T. Akita, T. Nakamura, M. Haruta, J. Catal. 209 (2002) 331.
[18] M.M. Mohamed, Appl. Catal. A 267 (2004) 135.
[19] B.M. Reddy, A. Khan, Catal. Surv. Asia 9 (3) (2005).
[20] S. Damyanova, C.A. Perez, M. Schmal, J.M.C. Bueno, Appl. Catal. A 234 (2002) 271.
[21] W. Chao-hail, T. Xin-hu, L. Jie-rong, T. Shu-ying, J. Environ. Sci. 19 (2007) 90.
[22] S. Sciré, S. Minico, C. Crisafulli, C. Satriano, A. Pistone, Appl. Catal. B 40 (2003) 43.
[23] Y. Lee, D. Kim, S. Shin, S. Oh, Mater. Chem. Phys. 100 (2006) 85.
[24] J. Sun, S. Fujita, F. Zhao, M. Hasegawa, M. Arai, J. Catal. 230 (2005) 398.
[25] A.C. Gluhoi, X. Tang, P. Marginean, B.E. Nieuwenhuys, Top. Catal. 39 (2006) 1.
[26] Y. Yang, S. Matsubara, M. Nogamia, J. Shi, Mater. Sci. Eng. B 140 (2007) 172.
[27] H. Huang, X. Yang, Colloids Surf. A: Eng. Asp. 255 (2005) 11.
[28] J. Zhu, Phys. Lett. A 339 (2005) 466.
[29] D. Andreeva, V. Idakiev, T. Tabakova, L. Ilieva, P. Falaras, A. Bourlinos, A. Travlos, Catal. Today 72 (2002) 51.
[30] G. Munteanu, L. Ilieva, R. Nedyalkova, D. Andreeva, Appl. Catal. A 277 (2004) 31.